

Dynamic dissipative cooling of a mechanical oscillator in strong-coupling optomechanics

Yong-Chun Liu^{1,2}, Yun-Feng Xiao^{1,*}, Xingsheng Luan², and Chee Wei Wong^{2†}

¹State Key Laboratory for Mesoscopic Physics and School of Physics,
Peking University, Beijing 100871, P. R. China and

²Optical Nanostructures Laboratory, Columbia University, New York, NY 10027, USA
(Dated: November 1, 2018)

Cooling of mesoscopic mechanical resonators represents a primary concern in cavity optomechanics. Here in the strong optomechanical coupling regime, we propose to dynamically control the cavity dissipation, which is able to significantly accelerate the cooling process while strongly suppressing the heating noise. Furthermore, the dynamic control is capable of overcoming quantum backaction and reducing the cooling limit by several orders of magnitude. The dynamic dissipation control provides new insights for tailoring the optomechanical interaction and offers the prospect of exploring macroscopic quantum physics.

PACS numbers: 42.50.Wk, 07.10.Cm, 42.50.Lc

One of the ultimate goals in quantum physics is to overcome the thermal noise, so that quantum effects can be observed experimentally. A prominent example is cavity optomechanics [1, 2], which enables not only the fundamental test of quantum theory and the exploration of quantum-classical boundary, but also important applications in quantum information processing and precision metrology. For these applications, the first crucial step is to prepare the mechanical resonator into the quantum regime [3–5]. So far, numerous experiments have focused on backaction cooling [6–12] in the weak optomechanical coupling regime, holding potential for ground-state preparation of mechanical resonators in the resolved sideband condition [13–15], along with backaction evading quantum non-demolition measurements [16–19]. Further step lies in the strong coupling, essential for coherent quantum optomechanical manipulations [5, 20–24] and electromechanical interactions [25, 26]. However, till date, strongly-coupled optomechanical cooling has predicted only limited improvement over weak coupling due to the saturation effect of the steady-state cooling rate [22, 27, 28]. Although strong coupling allows state swapping [5, 21], it cools the mechanical resonator only at a single instant in the Rabi oscillation cycle. Thus it is urgent to overcome these limitations for cooling and manipulating mesoscopic mechanical systems in the quantum regime.

For this purpose, in this Letter we show the dynamic tailoring of the cooling and heating processes by exploiting the cavity dissipation, overcoming the saturation of the steady-state cooling rate. This greatly accelerates the cooling process and thereby strongly suppresses the thermal noise. Moreover, heating induced by swapping and

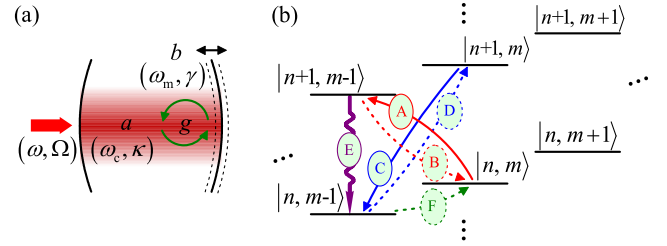


FIG. 1: (color) (a) Sketch of a typical optomechanical system. (b) Level diagram of the linearized Hamiltonian (1). $|n, m\rangle$ denotes the state of n photons and m phonons in the displaced frame. The solid (dashed) curves with arrows correspond to the cooling (heating) processes.

interaction quantum backaction are largely suppressed by periodic modulation of the cavity dissipation, which breaks the fundamental limitation of backaction cooling.

We consider a generic optomechanical system in which an optical cavity driven by a laser is coupled to a mechanical resonance mode, as illustrated in Fig. 1(a). In the rotating frame at the driven laser frequency ω , the system Hamiltonian reads $H = -(\omega - \omega_c)a^\dagger a + \omega_m b^\dagger b + ga^\dagger a(b + b^\dagger) + (\Omega a^\dagger + \Omega^* a)$ [29], where a (b) represents the annihilation operator for the optical (mechanical) mode with ω_c (ω_m) being the corresponding angular resonance frequency; g denotes the single-photon optomechanical coupling rate; Ω represents the driving strength. For strong driving, the Hamiltonian can be linearized, with $a \equiv a_1 + \alpha$, $b \equiv b_1 + \beta$. Here a_1 and b_1 describe the fluctuations around the mean values $\alpha \equiv \langle a \rangle$ and $\beta \equiv \langle b \rangle$, respectively. Neglecting the nonlinear terms, this yields the Hamiltonian

$$H_L = -\Delta' a_1^\dagger a_1 + \omega_m b_1^\dagger b_1 + (G a_1^\dagger + G^* a_1)(b_1 + b_1^\dagger), \quad (1)$$

where $\Delta' = \omega - \omega_c + 2|G|^2/\omega_m$ is the optomechanical-coupling modified detuning, and $G = \alpha g$ describes the linear coupling strength. Taking the dissipa-

*Corresponding author: yfxiao@pku.edu.cn;
www.phy.pku.edu.cn/~yfxiao/index.html

†Corresponding author: cww2014@columbia.edu

tions into consideration, the system is governed by the quantum master equation $\dot{\rho} = i[\rho, H_L] + \kappa\mathcal{D}[a_1]\rho + \gamma(n_{\text{th}} + 1)\mathcal{D}[b_1]\rho + \gamma n_{\text{th}}\mathcal{D}[b_1^\dagger]\rho$, where $\mathcal{D}[\hat{o}]\rho = \hat{o}\rho\hat{o}^\dagger - (\hat{o}^\dagger\hat{o}\rho + \rho\hat{o}^\dagger\hat{o})/2$ denotes the Liouvillian in Lindblad form for operator \hat{o} ; $\kappa \equiv \omega_c/Q_c$ ($\gamma \equiv \omega_m/Q_m$) represents the dissipation rate of the optical cavity (mechanical) mode; $n_{\text{th}} = 1/(e^{\hbar\omega_m/k_B T} - 1)$ corresponds to the thermal phonon number at the environmental temperature T .

Figure 1(b) displays the level diagram of H_L and the coupling routes among states $|n, m\rangle$ with n (m) being the photon (phonon) number in the displaced frame. We note that there are three kinds of heating processes denoted by the dashed curves in Fig. 1(b), corresponding to swap heating (B), quantum backaction heating (D) and thermal heating (F). Suppressing thermal heating is the ultimate goal while swap heating and quantum backaction heating are the accompanying effect when radiation pressure is utilized to cool the mechanical motion. Swap heating emerges when the system is in the strong coupling regime which enables reversible energy exchange between photons and phonons. Meanwhile, quantum backaction heating can pose a fundamental limit for backaction cooling. The solid curves (A , C and E) illustrate cooling processes associated with energy swapping, counter-rotating-wave interaction and cavity dissipation, which one seeks to enhance while suppressing heating for efficient mechanical motion cooling.

We focus on the resolved sideband regime $\kappa < \omega_m$ and we set $\Delta' = -\omega_m$, in which the beam splitter interaction $a_1^\dagger b_1 + a_1 b_1^\dagger$ is on resonance. In this case the dynamical stability condition from the Routh-Hurwitz criterion [30] requires $2|G| < \omega_m$. To realize cooling, the cooperativity $C \equiv 4|G|^2/(\gamma\kappa) \gg 1$ should also be satisfied. Starting from the master equation, we obtain a set of differential equations for the mean values of the second-order moments $\bar{N}_a = \langle a_1^\dagger a_1 \rangle$, $\bar{N}_b = \langle b_1^\dagger b_1 \rangle$, $\langle a_1^\dagger b_1 \rangle$, $\langle a_1 b_1 \rangle$, $\langle a_1^2 \rangle$ and $\langle b_1^2 \rangle$ (see Supplementary Material [31]). In the steady state we obtain the phonon occupancy [22, 27]

$$\bar{N}_{\text{std}} \simeq \frac{\gamma(4|G|^2 + \kappa^2)}{4|G|^2(\kappa + \gamma)} n_{\text{th}} + \frac{\kappa^2 + 8|G|^2}{16(\omega_m^2 - 4|G|^2)}, \quad (2)$$

where the first term is the classical cooling limit and the second term originates from the quantum backaction, consisting of both dissipation quantum backaction related to the cavity dissipation (with the associated fluctuation-dissipation theorem) and interaction quantum backaction associated with the optomechanical interaction (see Supplementary Material [31] for full description). In the weak coupling regime, Eq. (2) reduces to $\bar{N}_{\text{std}}^{\text{wk}} \simeq \gamma n_{\text{th}}/(\Gamma + \gamma) + \kappa^2/(16\omega_m^2)$ with $\Gamma = 4|G|^2/\kappa$, which agrees with Refs. [13, 14], and with $\kappa^2/(16\omega_m^2)$ the dissipation quantum backaction from fluctuation-dissipation. In the strong coupling regime, we obtain $\bar{N}_{\text{std}}^{\text{str}} \simeq \gamma n_{\text{th}}/(\kappa + \gamma) + |G|^2/[2(\omega_m^2 - 4|G|^2)]$. In this case

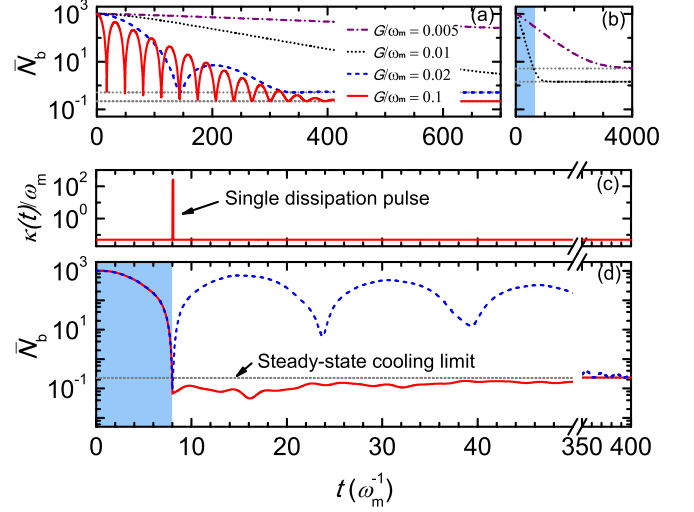


FIG. 2: (color) (a) Time evolution of mean phonon number \bar{N}_b for $G/\omega_m = 0.005, 0.01, 0.02$ and 0.1 (numerical results). (b) \bar{N}_b for $G/\omega_m = 0.005$ and 0.01 with a wider time interval. The shadowed region shows the same time interval with (a). (c) Modulation scheme of the cavity dissipation rate $\kappa(t)$ for fast cooling to the steady-state limit and (d) the time evolution of mean phonon number \bar{N}_b with (red solid curve) and without (blue dashed curve) modulation for $G/\omega_m = 0.2$. Other parameters: $n_{\text{th}} = 10^3$, $\gamma/\omega_m = 10^{-5}$, $\kappa/\omega_m = 0.05$. The dotted horizontal lines correspond to the steady-state cooling limits, given by Eq. (2).

the classical limit is restricted by the cavity dissipation rate κ , while the interaction quantum backaction limit suffers from high coupling rate $|G|$.

To study the cooling dynamics beyond the steady state, we solve the differential equations to obtain the time evolution of the mean phonon number \bar{N}_b . For weak coupling, we have $\bar{N}_b^{\text{wk}} \simeq n_{\text{th}}(\gamma + \Gamma e^{-\Gamma t})/(\gamma + \Gamma) + [\kappa^2/(16\omega_m^2)](1 - e^{-\Gamma t})$, which shows that the mean phonon number decays exponentially with the cooling rate Γ . This cooling rate is limited by the coupling strength, since in the cooling route $A \rightarrow E$ the energy flow from the mechanical mode to the optical mode (process A) is slower than the cavity dissipation (process E).

In the strong coupling regime, we obtain the time evolution of the mean phonon number described by (see Supplementary Material [31])

$$\begin{aligned} \bar{N}_b^{\text{str}} &= \bar{N}_{b,1}^{\text{str}} + \bar{N}_{b,2}^{\text{str}}, \quad (3) \\ \bar{N}_{b,1}^{\text{str}} &\simeq n_{\text{th}} \frac{\gamma + \frac{1}{2} e^{-\frac{\kappa+\gamma}{2}t} [\kappa - \gamma + (\kappa + \gamma) \cos(\omega_+ - \omega_-)t]}{\kappa + \gamma}, \\ \bar{N}_{b,2}^{\text{str}} &\simeq \frac{|G|^2 \left[1 - e^{-\frac{\kappa+\gamma}{2}t} \cos(\omega_+ + \omega_-)t \cos(\omega_+ - \omega_-)t \right]}{2(\omega_m^2 - 4|G|^2)}, \end{aligned}$$

where $\omega_{\pm} = \sqrt{\omega_m^2 \pm 2|G|\omega_m}$ are the normal eigenmode frequencies. The phonon occupancy exhibits oscillation under an exponentially-decaying envelope and can be di-

vided into two distinguished parts $\bar{N}_{b,1}^{\text{str}}$ and $\bar{N}_{b,2}^{\text{str}}$, where the first part originates from energy exchange between optical and mechanical modes, and the second part is induced by quantum backaction. $\bar{N}_{b,1}^{\text{str}}$ reveals Rabi oscillation with frequency $\sim 2|G|$, whereas the envelopes have the same exponential decay rate $\Gamma' = (\kappa + \gamma)/2$ regardless of the coupling strength $|G|$. This is because, in the strong coupling regime, the cooling route $A \rightarrow E$ is subjected to the cavity dissipation (process E), which has slower rate than the energy exchange between phonons and photons (process A). This saturation prevents a higher cooling speed for stronger coupling. In Figs. 2(a) and (b) we plot the numerical results based on the master equation for various G . It shows that for weak coupling the cooling rate increases rapidly as the coupling strength increases, whereas for strong coupling the envelope decay no longer increases, instead the oscillation frequency becomes larger.

Fast cooling to the steady-state limit.—To speed up the cooling process in the strong coupling regime, here we take advantage of high cavity dissipation to dynamically strengthen the cooling process E . The internal cavity dissipation is abruptly increased each time when the Rabi oscillation reaches a minimum-phonon state, such as through RF-synchronized carrier injection to the optical cavity [32]. At this time the system has transited from state $|n, m\rangle$ to state $|n+1, m-1\rangle$. Once a strong dissipation pulse is applied to the cavity so that the process E dominates, the system will irreversibly transit from state $|n+1, m-1\rangle$ to state $|n, m-1\rangle$. The dissipation pulse has essentially behaves as a switch to halt the reversible Rabi oscillation, resulting in the suppression of the swap heating. To verify this dissipative cooling, in Figs. 2 (c) and (d) we plot the modulation scheme and the corresponding time evolution of mean phonon number \bar{N}_b for $\kappa/\omega_m = 0.05$ and $G/\omega_m = 0.2$. At the end of the first half Rabi oscillation cycle, $t \sim \pi/(2|G|)$, a dissipation pulse of pulsewidth $0.01\pi/(2|G|)$ is applied. Detailed tradeoffs of the dissipation quantum backaction and the interaction quantum backaction for varying pulsewidths are shown in the Supplementary Material [31]. After incidence of the dissipation pulse, the phonon number reaches and remains near the steady-state limit. For short time scales, the remaining small-amplitude oscillations mainly originate from counter-rotating-wave interactions. Note that without modulation (blue dashed curve), the steady-state cooling limit is reached only after $t \simeq 400/\omega_m$; while with the modulation (red solid curve), it only takes $t \simeq 8/\omega_m$ to cool below the same limit.

Breaking the fundamental limit of backaction cooling.—By periodically modulating the cavity dissipation so as to continuously suppress the swap heating, the phonon occupancy can be kept below the steady-state cooling limit. Actually, each time after the dissipation pulse is applied, the photon number quickly drops to the vacuum state, which equivalently re-initializes the system.

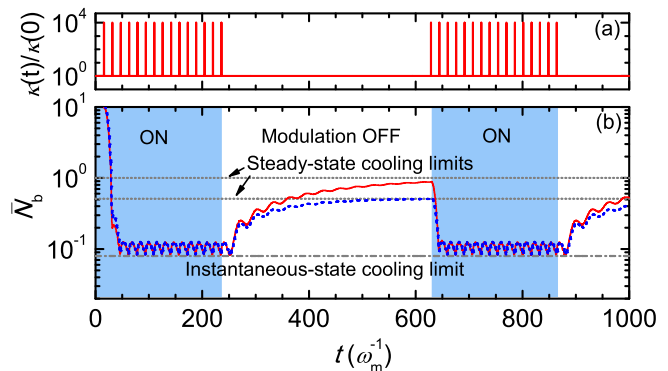


FIG. 3: (color) Modulation scheme of $\kappa(t)/\kappa(0)$ (a) and the corresponding time evolution of \bar{N}_b (b) for $G/\omega_m = 0.1$, $\kappa(0)/\omega_m = 0.01$ (red solid curve) and 0.02 (blue dashed curve). In (b), the two dotted horizontal lines (from top to bottom) denoting the respective steady-state cooling limits depending on the cavity decay $\kappa(0)$, given by Eq. (2); the dash-dotted line denotes the instantaneous-state cooling limit independent of $\kappa(0)$, given by Eq. (4); the “ON” and “OFF” regions corresponds that the modulation is turned on and off, respectively; the vertical coordinate range from 10 to 10^3 is not shown. Other parameters: $n_{\text{th}} = 10^3$, $\gamma/\omega_m = 10^{-5}$.

By periodic pulse application, the system will periodically re-initializes, which keeps the phonon occupancy in an instantaneous-state cooling limit as verified in Fig. 3. The instantaneous-state cooling limit is given by (see Supplementary Material [31])

$$\bar{N}_{\text{ins}} \simeq \frac{\pi\gamma n_{\text{th}}}{4|G|} + \frac{\pi^2 |G|^4}{(\omega_m^2 - |G|^2)(\omega_m^2 - 4|G|^2)}. \quad (4)$$

Here the first term comes from $\bar{N}_{b,1}^{\text{str}}$ for $t \simeq \pi/(2|G|)$, which shows a $\pi\kappa/(4|G|)$ times reduction of classical steady-state cooling limit. The second term of $\sim \pi^2 |G|^4/\omega_m^4$, obtained from $\bar{N}_{b,2}^{\text{str}}$ when $t \simeq \pi/\omega_m$, reveals that the second order term of $|G|/\omega_m$ in quantum backaction has been removed in our approach, leaving only the higher-order terms. Note that the cooling limit (4) is the sum of the individual minimum of $\bar{N}_{b,1}^{\text{str}}$ and $\bar{N}_{b,2}^{\text{str}}$ in their first oscillation cycle. Notably, in Fig. 3 we demonstrate that the modulation is switchable. If we turn on the modulation (“ON” region), the system will reach the instantaneous-state cooling limit; if we turn off the modulation (“OFF” region), the system transits back to the steady-state cooling limit.

In particular, from Eq. (3), the interaction quantum backaction heating term $\bar{N}_{b,2}^{\text{str}}$ forms a carrier-envelope type evolution, where the carrier oscillation represents the counter-rotating-wave interaction and the envelope oscillation is a result of coherent energy exchange due to strong coupling. The minimum of $\bar{N}_{b,2}^{\text{str}}$ is dependent on the carrier-envelope frequency matching. If $(\omega_+ + \omega_-)/(\omega_+ - \omega_-) = k$ ($k = 3, 5, \dots$), yielding $|G|/\omega_m = k/(k^2 + 1) = 0.3, 5/26, \dots$, $\bar{N}_{b,2}^{\text{str}}$ reaches a mini-

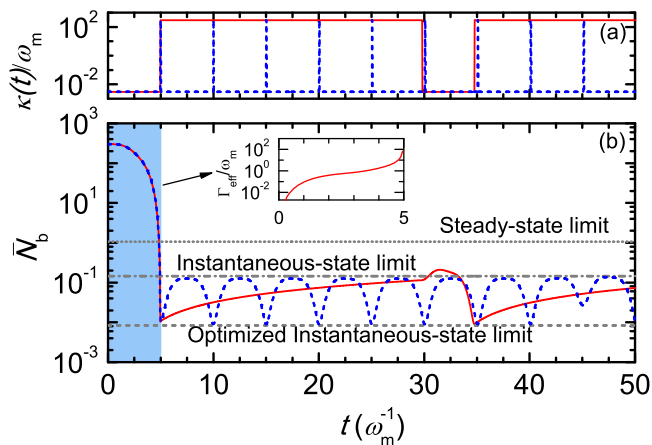


FIG. 4: (color) Different pulsewidth (a) and the corresponding time evolution (b) of \bar{N}_b . The horizontal lines indicate the three cooling limits given by Eqs. (2), (4) and (5) from top to bottom. The inset shows the effective cooling rate as a function of time. Parameters : $n_{\text{th}} = 300$, $G/\omega_m = 0.3$, $\kappa/\omega_m = 0.003$ and $\gamma/\omega_m = 10^{-5}$.

mum $\sim \frac{\pi\kappa|G|}{8(\omega_m^2 - 4|G|^2)}$ for $t \simeq \pi/(2|G|)$. Here we obtain the optimized instantaneous-state cooling limit as ([31])

$$\bar{N}_{\text{ins}}^{\text{opt}} \simeq \frac{\pi\kappa}{4|G|} \left[\frac{\gamma n_{\text{th}}}{\kappa} + \frac{|G|^2}{2(\omega_m^2 - 4|G|^2)} \right], \quad (5)$$

which reduces both the classical and quantum steady-state cooling limits by a factor of $\pi\kappa/(4|G|)$. Remarkably, this reduction is significant when the system is in the deep strong coupling regime. Besides, the leading order of the interaction quantum backaction heating scales as $\kappa|G|/\omega_m^2$, which can be a few orders of magnitude lower than the steady-state case, representing large suppression of quantum backaction.

To verify suppression of the interaction quantum backaction heating, in Fig. 4 we plot the cooling dynamics with dissipation modulation for $G/\omega_m = 0.3$ and $\kappa/\omega_m = 0.003$. The single modulation pulse brings down the phonon occupation to the optimized instantaneous-state cooling limit described in Eq. (5), with the time-dependent effective cooling rate $\Gamma_{\text{eff}} = (d\bar{N}_b/dt)/\bar{N}_b$ shown in the inset. With short-pulse modulation (blue dashed curve), the remaining oscillation, mainly induced by the counter-rotating-wave interaction, has a quasi-period of $\pi/(2|G|)$ due to frequency matching. This small-amplitude fluctuations around the instantaneous-state cooling limit might affect future quantum protocols, but in the sense of time-averaged through timescales larger than $\pi/(2|G|)$, the cooling limit can be viewed stable. By using long-pulse modulation, the quasi-periodic fluctuations can be suppressed (red solid curve). This is because the large dissipation suppresses the interaction quantum backaction. The cost is that the dissipation quantum backaction takes effect and gradually increases

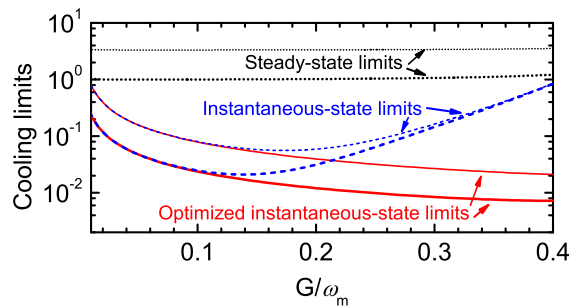


FIG. 5: (color) Cooling limits given by Eqs. (2) (black dotted curves), (4) (blue dashed curves) and (5) (red solid curves) versus G/ω_m for $n_{\text{th}} = 10^3$ (thin curves), 3×10^2 (thick curves). Other parameters are $\kappa/\omega_m = 0.003$ and $\gamma/\omega_m = 10^{-5}$.

the phonon number. This trade-off can be balanced by optimizing the pulsewidth as shown in the Supplementary Material [31].

Figure 5 plots the cooling limits as functions of G/ω_m , which reveals that instantaneous-state cooling limits are much lower than steady-state cooling limits. For small coupling rates, we observed that interaction quantum backaction is insignificant and suppression of swap heating is the main origin of cooling limit reduction. For large coupling rates, suppressing interaction quantum backaction is crucial for obtaining lower limits. Typically, the cooling limits can be reduced by a few orders of magnitude. For example, when $G/\omega_m = 0.3$ and $\kappa/\omega_m = 0.003$, we obtain $\bar{N}_{\text{std}} = 3.4$, while $\bar{N}_{\text{ins}}^{\text{opt}} = 0.03$, corresponding to more than 100 times of phonon number suppression.

Experimentally, the dynamic control of cavity dissipation can be realized, for example, by modulating free-carrier plasma density [32–34] or using a light absorber/scatterer [35]. Note that we assume G is kept unchanged when the dissipation pulses are applied, which corresponds to the invariableness of the intracavity field α . This can be fulfilled by simultaneously changing the driving $\Omega(t)$, so that equation $[i\Delta' - \kappa(t)/2]\alpha - i\Omega(t) = 0$ is satisfied all the time ([31]; Section VI). Here modulated square-shaped dissipation pulses are used though further simulations show that the results are irrespective of the pulse shape, as long as they are executed quickly with strong enough peak value at the desired time. This is because the pulse dissipation mainly relies on the pulse area.

In summary, we examined cooling of mesoscopic mechanical resonators in the strong coupling regime and propose dynamic dissipative schemes which possess large cooling rates, low cooling limits, and long-time stability. By making use of the cavity dissipation, swap heating can be strongly avoided and the interaction quantum backaction largely suppressed, with great advantages over the current conventional cooling approaches. For example, a single dissipation pulse enables more than 50 times

higher cooling rate; with periodic modulation of cavity dissipation, the cooling limit can be reduced by more than two orders of magnitude. Different from the cooling schemes with modulated coupling [36–40], we take advantage of large cavity dissipation, usually regarded as a noise source. Together with recent proposals of other dissipative effects such as two-level ensembles [41] or photothermal effect [42, 43], we demonstrate that cavity dissipation (even in the presence of the considered dissipation quantum backaction) can be viewed as a resource. Compared with the dissipative coupling [44–46], this active dissipation control does not require the coupling between the cavity dissipation and the mechanical resonator. The dynamic dissipative cooling provides a new way for exploring the quantum regime of mechanical devices, ranging from mechanical ground state preparation, to generation of mesoscopic quantum states, and quantum-limited measurements.

We thank H.-K. Li for discussions. This work is supported by DARPA ORCHID program (C11L10831), 973 program (2013CB328704 and 2013CB921904), NSFC (11004003, 11222440, and 11121091), and RFDPH (20120001110068). Y.C.L is supported by the PhD Students' Short-term Overseas Research Program of Peking University and Scholarship Award for Excellent Doctoral Candidates.

-
- [1] T. J. Kippenberg and K. J. Vahala, *Science* **321**, 1172 (2008).
- [2] F. Marquardt and S. M. Girvin, *Physics* **2**, 40 (2009).
- [3] J. D. Teufel *et al.*, *Nature (London)* **475**, 359 (2011).
- [4] J. Chan *et al.*, *Nature (London)* **478**, 89 (2011).
- [5] E. Verhagen, S. Deléglise, S. Weis, A. Schliesser, and T. J. Kippenberg, *Nature (London)* **482**, 63 (2012).
- [6] S. Gigan *et al.*, *Nature (London)* **444**, 67 (2006).
- [7] O. Arcizet, P.-F. Cohadon, T. Briant, M. Pinard, and A. Heidmann, *Nature (London)* **444**, 71 (2006).
- [8] A. Schliesser, R. Rivière, G. Anetsberger, O. Arcizet, and T. J. Kippenberg, *Nature Phys.* **4**, 415 (2008).
- [9] S. Gröblacher *et al.*, *Nature Phys.* **5**, 485 (2009).
- [10] Y.-S. Park and H. Wang, *Nature Phys.* **5**, 489 (2009).
- [11] A. Schliesser, O. Arcizet, R. Rivière, G. Anetsberger, and T. J. Kippenberg, *Nature Phys* **5**, 509 (2009).
- [12] T. Rocheleau *et al.*, *Nature (London)* **463**, 72 (2010).
- [13] I. Wilson-Rae, N. Nooshi, W. Zwerger, and T. J. Kippenberg, *Phys. Rev. Lett.* **99**, 093901 (2007).
- [14] F. Marquardt, J. P. Chen, A. A. Clerk, and S. M. Girvin, *Phys. Rev. Lett.* **99**, 093902 (2007).
- [15] C. Genes, D. Vitali, P. Tombesi, S. Gigan, and M. Aspelmeyer, *Phys. Rev. A* **77**, 033804 (2008).
- [16] J. B. Hertzberg *et al.*, *Nature Phys.* **77**, 213 (2010).
- [17] M. R. Vanner *et al.*, *Proc. Natl. Acad. Sci.* **77**, 16182 (2011).
- [18] Braginsky, *JETP Lett.* **27**, 276 (1978).
- [19] Braginsky, *Quantum Measurements* (Cambridge University Press, Cambridge, 1978).
- [20] S. Gröblacher, K. Hammerer, M. R. Vanner, and M. Aspelmeyer, *Nature (London)* **460**, 724 (2009).
- [21] T. A. Palomaki, J. W. Harlow, J. D. Teufel, R. W. Simmonds, and K. W. Lehnert, arXiv:1206.5562.
- [22] J. M. Dobrindt, I. Wilson-Rae, and T. J. Kippenberg, *Phys. Rev. Lett.* **101**, 263602 (2008).
- [23] S. Huang and G. S. Agarwal, *Phys. Rev. A* **80**, 033807 (2009).
- [24] U. Akram, N. Kiesel, M. Aspelmeyer and G. J. Milburn, *New J. Phys.* **12**, 083030 (2010).
- [25] A. D. O'Connell *et al.*, *Nature (London)* **464**, 697 (2010).
- [26] J. M. Taylor, A. S. Sørensen, C. M. Marcus, and E. S. Polzik, *Phys. Rev. Lett.* **107**, 273601 (2011).
- [27] I. Wilson-Rae, N. Nooshi, J. Dobrindt, T. J. Kippenberg and W. Zwerger, *New J. Phys.* **10**, 095007 (2008).
- [28] P. Rabl, C. Genes, K. Hammerer, and M. Aspelmeyer, *Phys. Rev. A* **80**, 063819 (2009).
- [29] C. K. Law, *Phys. Rev. A* **51**, 2537 (1995).
- [30] R. Ghobadi, A. R. Bahrapour, and C. Simon, *Phys. Rev. A* **84**, 033846 (2011).
- [31] Supplementary Material online.
- [32] Q. Xu, P. Dong, and M. Lipson, *Nature Phys.* **3**, 406 (2007).
- [33] K. Kondo *et al.*, *Phys. Rev. Lett.* **110**, 053902 (2013).
- [34] R. A. Soref and B. R. Bennett, *IEEE J. Quantum Electron.* **23**, 123 (1987).
- [35] I. Favero and K. Karrai, *New J. Phys.* **10**, 095006 (2008).
- [36] L. Tian, *Phys. Rev. B* **79**, 193407 (2009).
- [37] Y. Li, L.-A. Wu, and Z. D. Wang, *Phys. Rev. A* **83**, 043804 (2011).
- [38] J.-Q. Liao and C. K. Law, *Phys. Rev. A* **84**, 053838 (2011).
- [39] X. Wang, S. Vinjanampathy, F. W. Strauch, and K. Jacobs, *Phys. Rev. Lett.* **107**, 177204 (2011).
- [40] S. Machnes *et al.*, *Phys. Rev. Lett.* **108**, 153601 (2012).
- [41] C. Genes, H. Ritsch, and D. Vitali, *Phys. Rev. A* **80**, 061803(R) (2009).
- [42] J. Restrepo, J. Gabelli, C. Ciuti, and I. Favero, *Comptes Rendus Physique* **12**, 860 (2011).
- [43] S. D. Liberato, N. Lambert, and F. Nori, *Phys. Rev. A* **83**, 033809 (2011).
- [44] F. Elste, S. M. Girvin, and A. A. Clerk, *Phys. Rev. Lett.* **102**, 207209 (2009).
- [45] A. Xuereb, R. Schnabel, and K. Hammerer, *Phys. Rev. Lett.* **107**, 213604 (2011).
- [46] M. Li, W. H. P. Pernice, and H. X. Tang, *Phys. Rev. Lett.* **103**, 223901 (2009).